

# Dark Matter and the CACTUS Gamma-Ray Excess from Draco

Stefano Profumo and Marc Kamionkowski

*California Institute of Technology, Pasadena, CA 91125, USA*

E-mail: profumo@caltech.edu, kamion@tapir.caltech.edu

## Abstract

The CACTUS atmospheric Cherenkov telescope collaboration recently reported a gamma-ray excess from the Draco dwarf spheroidal galaxy. Draco features a very low gas content and a large mass-to-light ratio, suggesting as a possible explanation annihilation of weakly interacting massive particles (WIMPs) in the Draco dark-matter halo. We show that with improved angular resolution, future measurements can determine whether the halo is cored or cuspy, as well as its scale radius. We find the relevant WIMP masses and annihilation cross sections and show that supersymmetric models can account for the required gamma-ray flux. The annihilation cross section range is found to be not compatible with a standard thermal relic dark-matter production. We compute for these supersymmetric models the resulting Draco gamma-ray flux in the GLAST energy range and the rates for direct neutralino detection and for the flux of neutrinos from neutralino annihilation in the Sun. We also discuss the possibility that the bulk of the signal detected by CACTUS comes from direct WIMP annihilation to two photons and point out that a decaying-dark-matter scenario for Draco is not compatible with the gamma-ray flux from the Galactic center and in the diffuse gamma-ray background.

---

## Contents

<b>1</b>	<b>Introduction</b>	<b>1</b>
<b>2</b>	<b>The dark-matter halo of Draco</b>	<b>3</b>
<b>3</b>	<b>The CACTUS excess and dark matter</b>	<b>6</b>
3.1	The gamma-ray angular distribution . . . . .	8
3.2	Implications for particle dark matter . . . . .	10
3.3	Supersymmetric dark matter . . . . .	13
3.4	Monochromatic gamma rays . . . . .	17
3.5	Decaying dark matter . . . . .	20
<b>4</b>	<b>Conclusions</b>	<b>21</b>

---

## 1 Introduction

Despite compelling indirect astrophysical and cosmological evidence, the fundamental nature of non-baryonic dark matter remains elusive (see Refs. [1, 2] for recent reviews). Upgrades of direct detectors looking for scattering of dark-matter particles from nuclei, future neutrino telescopes, and space-based antimatter and gamma-ray detectors will dramatically enhance the possibility to discover dark-matter particles in the Galactic halo. Given our complete ignorance on the nature of dark matter, any anomalous experimental result that might point to dark matter should be carefully analyzed, and possibly cross-correlated both with other observational constraints and with existing theoretical models.

Among indirect-detection techniques that seek products of dark-matter annihilations, those searching for neutrinos and photons play a special role. Unlike electrically charged particles, like antiprotons or positrons, which diffuse in the Galactic magnetic field, the arrival direction of neutrinos and photons points to where the dark-matter annihilation took place. In particular, the forthcoming launch of the Gamma Ray Large Area Space Telescope (GLAST) [3] and the rapidly developing field of ground based Atmospheric Cherenkov Telescopes (ACTs) [4] make the search for energetic photons from dark-matter annihilation a particularly promising and exciting endeavor.

Since the rate per unit volume for dark-matter annihilation depends on the square of the dark-matter density, there may be great advantage to seeking astrophysical locations where the dark-matter density is believed to be high. The center of the Milky Way has been viewed as a promising target as it might host a dark-matter spike and/or because the Galactic halo could feature a steep cusp towards its center [5]. On the other hand, diffuse gamma-ray backgrounds produced by the spallation of cosmic rays on interstellar gas, and the uncertainties on the distribution of molecular hydrogen in the galactic ridge, may blur the dark-matter-induced signal (but for a different viewpoint see Ref. [6]). The presence of other gamma-ray emitters in the central region of our Galaxy, including those associated with the supermassive central black hole and the supernova remnant Sgr A\*, however, also make it difficult to distinguish a putative dark-matter signal and its astrophysical background [7, 8].

It has therefore been suggested that one should instead seek dark-matter-induced gamma rays from other sources that feature large dark-matter densities but that remain devoid of background sources. In particular, several extragalactic sources have been considered [9, 10, 11, 12, 13]. Among these, dwarf spheroidal (dSph) galaxies are among the most dark-matter dominated systems, featuring mass-to-light ratios as high as  $M/L \sim 250 M_{\odot}/L_{\odot}$  [14]. Moreover, at least four dSph galaxies with very large  $M/L$  lie within 100 kpc from the Milky Way center.

The dark-matter-induced photon flux depends on the dark-matter distribution, and particularly on its inner structure, which is unfortunately poorly known in the case of local dSphs. Ref. [10] modeled the dark-matter halos of the four nearby dSph, Carina, Draco, Ursa Minor, and Sextans, with King profiles. Even with optimistic assumptions on the background-rejection capabilities of ACTs, they found that the gamma-ray flux expected from supersymmetric models from local dSphs is typically at least three orders of magnitude below the background. They find that if the dark-matter distribution is clumpy, the signal can be boosted by at most a factor of 40, which would still be insufficient. A re-examination of the Draco dSph galaxy in Ref. [9] arrived at somewhat different conclusions. This work showed that, assuming a steeply cusped isothermal dark-matter halo, a large portion of the supersymmetric parameter space could produce a signal visible at both forthcoming ACTs and at GLAST. This work also pointed out that, depending on the magnetic-field strength inside Draco, the radio-continuum limits for Draco obtained in Ref. [15] could also rule out sizeable portions of the same parameter space. Ref. [11] conducted an extensive analysis of the 44 nearest galaxies in the Local Group, pointing out other promising extragalactic candidates, such as M31. A systematic comparison between the case of the Galactic center and that of various nearby dSph galaxies (Sagittarius, Draco, and Canis Major) was carried out in Ref. [13], where a wide array of halo profiles was also employed. Depending on the latter, Ref. [13] concludes that if dark matter is supersymmetric, dSph galaxies may indeed produce a detectable signal in ACTs and at GLAST.

Recently, a gamma-ray excess from the direction of Draco has been detected by the Solar 2 Heliostat

Array CACTUS, located in Barstow, California [16]. Although the robustness of the signal has still to be tested, the possibility of ascribing the excess over the off-source background to dark-matter annihilation in Draco’s halo is certainly intriguing, as Draco is a dark-matter dominated system (see Sec. 2) that is not expected to host any other significant gamma-ray source [9, 17]. This possibility was recently envisaged in Ref. [18]. In the present analysis, we study the impact on the gamma-ray flux of various, astrophysically motivated, halo models [19]. We point out that if the angular resolution of the experiment can be improved and understood, then measurement of the angular distribution of the gamma-ray excess can discriminate between cuspy (e.g., the Navarro-Frenk-White profile [20]) and cored profiles and determine the halo scale radius (Sec. 3.1). In the absence of a full analysis of the raw counts reported by CACTUS [16], the estimate of the flux of photons to be attributed to dark-matter annihilation appears particularly critical. Here, we conservatively estimate the putative gamma-ray flux detected by CACTUS [16] bracketing it between an upper estimate where all the CACTUS excess counts over the background are attributed to the dark-matter signal (following the approach of Ref. [18]), and a lower estimate where only the counts in the innermost angular region are supposed to originate from dark-matter annihilations. We then scrutinize the dark-matter interpretation of the CACTUS excess from Draco on model-independent grounds on the planes defined by the particle mass and annihilation cross section (Sec. 3.2). We specialize to the particular case of supersymmetric dark matter in Sec. 3.3, where we also make predictions for the expected detection rates for models consistent with the Draco excess with other dark-matter searches. We consider in Sec. 3.4 the possibility that the bulk of the excess photons detected by CACTUS come from the monochromatic  $\gamma\gamma$  line. In Sec. 3.5, we show that the signal cannot come from the decay of a very long-lived dark species. We finally draw our conclusions in Sec. 4.

## 2 The dark-matter halo of Draco

Draco was the first dSph galaxy to show evidence of a large dark-matter content. A total mass much larger than the amount of visible matter was inferred in Ref. [21] from the measurement of four carbon stars in Draco as early as 1983. A few years later, the assessment of the velocities of 15 more stars allowed Ref. [22] to compute a mass-to-light ratio larger than  $50 M_{\odot}/L_{\odot}$ , a result subsequently confirmed by a much larger sample of 91 Draco stars in Ref. [23] and 17 stars in Ref. [24]. More recently, the existence of an extended dark-matter halo was inferred in Refs. [25, 26] from a sample of radial velocities of 159 giant stars out to large projected radii; the previously assumed hypothesis that mass follows light was shown to be inconsistent at the  $2.5\text{-}\sigma$  confidence level, and tentative evidence for a nearly isothermal dark-matter distribution was provided. A new re-evaluation of the Draco dark-matter distribution, based on new data [27] and on two-component high-resolution N-

body simulations, together with cosmological predictions for the properties of dark-matter halos, lead Ref. [19] to a few important conclusions, relevant for the present discussion. First, it was pointed out that both a cored and a cuspy profile are compatible with the observational data on Draco and with the results of numerical simulations. Second, the possibility that Draco is a tidal dwarf (i.e., a virtually unbound stellar stream tidally disrupted in the Milky Way gravitational potential [28]) was ruled out. This might very well be in contrast with other local dwarf galaxies [19, 13], for which a smaller amount of data is available.

The analysis of Ref. [19] assumes two types of (spherical) dark-matter halos. The first one, motivated by  $N$ -body simulations, is the well known Navarro-Frenk-White (NFW) density profile [20],

$$\rho_{\text{NFW}}(r) = \frac{\rho_s}{(r/r_s)(1+r/r_s)^2}, \quad (1)$$

as a function of radius  $r$ , while the second is the observationally motivated Burkert profile [29],

$$\rho_{\text{Bur}}(r) = \frac{\rho_s}{(1+r/r_s)[1+(r/r_s)^2]}. \quad (2)$$

The flux of gamma rays induced by dark-matter annihilation is clearly very sensitive to the parameters entering the two profiles; i.e. the scaling density ( $\rho_s$ ) and scale radius ( $r_s$ ). The  $(\rho_s, r_s)$  plane is constrained by observations as well as cosmological arguments. We reproduce in Fig. 1 with gray shading the viable portions on the  $(\rho_s, r_s)$  plane determined in Ref. [19]. The leftmost region is ruled out by the requirement that the dark-matter halo formed early enough to allow the subsequent formation of the bulk of its stellar component. The upper-right limit results from the requirement that the number of dSph galaxies in the Local group is equal at least to the number of observed objects. Finally, the viable region is bounded from below by the condition that Draco's virial radius extends out at least to the last observed point in its surface-brightness profile and by consistency with the observed line-of-sight stellar velocity dispersion. We indicate with blue crosses points corresponding to models that have  $\chi^2 < 9.5$  between the modeled and observed line-of-sight velocity-dispersion profiles according to the analysis of Ref. [19]. For future convenience, we pick four benchmark halo models, among those analyzed in Ref. [19], that feature a wide range of  $\rho_s$  and  $r_s$ ; we highlight these models in Fig. 1 with red squares. We collect the scaling densities and radii, as well as the values of  $J_{-3}$  and  $J_{-5}$  for the four benchmark models, in Table 1.

The observed integral flux of gamma rays with energies  $E > E_\gamma$  from dark-matter annihilation per unit solid angle is

$$\phi^{E_\gamma} \equiv \frac{N_\gamma \langle \sigma v \rangle}{4\pi m_{\text{DM}}^2} J_{\Delta\Omega}, \quad (3)$$

and depends on the particle mass  $m_{\text{DM}}$ , on its annihilation cross section  $\langle \sigma v \rangle$ , on the number  $N_\gamma$  of photons with energies  $E > E_\gamma$  produced per annihilation, and on the integral  $J_{\Delta\Omega}$  along the line of

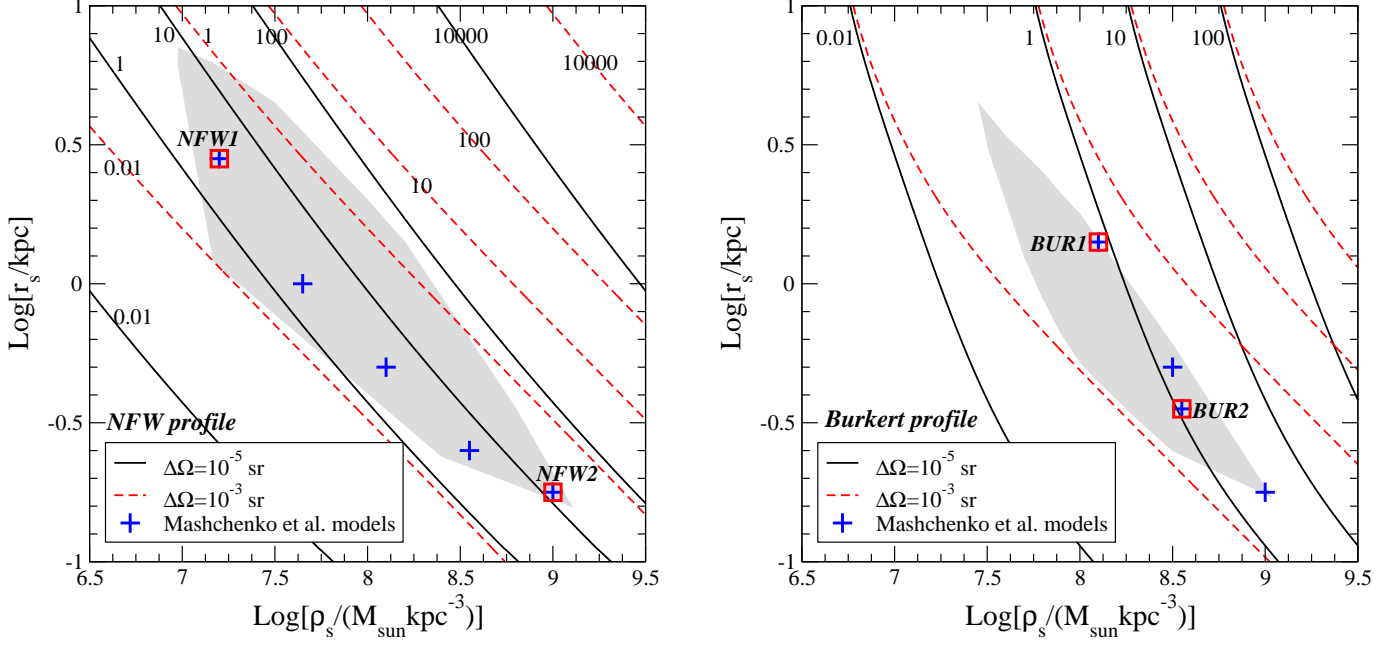


Figure 1: Curves of constant line-of-sight integral of the square of the dark-matter density  $J_{\Delta\Omega}$  (see Eq. (4) for the definition of this quantity), for  $\Delta\Omega = 10^{-5}$  (solid black lines) and  $\Delta\Omega = 10^{-3}$  (dashed red lines), on the  $(\rho_s, r_s)$  plane. For an NFW (left) and for a Burkert (right) dark-matter halo, gray regions correspond to cosmologically allowed ranges of the two halo parameters, while models indicated with blue crosses also give consistent simulated stellar velocity dispersions. We highlight with red squares the four benchmark halo models of Table 1.

sight of the square of the dark-matter density, averaged over the solid angle  $\Delta\Omega$  of the detector,

$$J_{\Delta\Omega} \equiv \frac{1}{\Delta\Omega} \int_{\Delta\Omega} \int_{\text{l.o.s.}} \rho_{\text{DM}}^2[r(s)] ds = \frac{2\pi}{\Delta\Omega} \int_0^{\theta_{\text{max}}} d\theta \sin\theta \int_{s_{\text{min}}}^{s_{\text{max}}} ds \rho_{\text{DM}}^2 \left( \sqrt{s^2 + s_0^2 - 2ss_0 \cos\theta} \right), \quad (4)$$

where

$$\theta_{\text{max}} \equiv \text{ArcCos} \left( 1 - \frac{\Delta\Omega}{2\pi} \right), \quad (5)$$

$$s_{\text{min, max}} \equiv s_0 \cos\theta \pm \sqrt{r_t^2 + s_0^2 \sin^2\theta}, \quad (6)$$

$s_0 = 75.8 \pm 0.7 \pm 5.4$  kpc being Draco's heliocentric distance, and  $r_t$  its tidal radius. The latter was evaluated, following the approach of Ref. [13], according to the Roche criterion (the radius such that the average mass in the dSph is equal to the average interior mass in the Milky Way halo); different tidal radii correspond to different Milky Way (and, though more weakly, to different Draco) dark-matter halos, ranging within less than one order of magnitude. However, since  $J_{\Delta\Omega}$  depends quite weakly on  $r_t \gg r_s$ , we resorted to an isothermal profile for the Milky Way, which typically gives  $r_t \approx 7$  kpc.

<b>Model</b>	$\log[\rho_s/(M_\odot \text{ kpc}^{-3})]$	$\log[r_s/\text{kpc}]$	$J_{-3}$	$J_{-5}$
<b>NFW1</b>	7.20	0.45	0.12	3.00
<b>NFW2</b>	9.00	-0.75	0.17	13.0
<b>BUR1</b>	8.10	0.15	0.26	0.75
<b>BUR2</b>	8.55	-0.45	0.05	1.13

Table 1: *Input parameters and line-of-sight integrals for four benchmark Draco halo models from Ref. [19].*

We show in Fig. 1 iso-level curves for the quantities  $J_{-3} \equiv J_{\Delta\Omega=10^{-3} \text{ sr}}$  and  $J_{-5}$ , relevant, respectively, for the full one-degree angular region where the gamma-ray excess from Draco was observed and for the innermost 0.1-degree angular region, where the largest dark-matter-induced gamma-ray flux is expected, on the  $(\rho_s, r_s)$  plane, for the NFW profile (left) and for the Burkert profile (right). We define here and the remainder of the paper the quantities  $J_{\Delta\Omega}$  in units of  $10^{23} \text{ GeV}^2 \text{ cm}^{-5}$ . We note that (1) the observationally and cosmologically consistent range for  $J_{-5}$  spans roughly one order of magnitude in the case of a cored profile and 2 orders of magnitude for a cuspy profile. (2) The ratio  $J_{-3}/J_{-5} \approx 1$  grows significantly with  $r_s$  for cored profiles, while  $J_{-3}/J_{-5} \approx 10 \div 100$  for cuspy profiles, with smaller values corresponding to larger scale radii. We find as a consistent range for  $J_{-5}$  (again in units of  $10^{23} \text{ GeV}^2 \text{ cm}^{-5}$ ),

$$0.11 \lesssim J_{-5} \lesssim 2.96, \quad \text{Burkert profile,}$$

$$0.35 \lesssim J_{-5} \lesssim 64.3, \quad \text{NFW profile.}$$

### 3 The CACTUS excess and dark matter

The CACTUS ACT observed a gamma-ray excess over background from an angular region extending approximately 1 degree around the direction of the Draco dwarf spheroidal galaxy [16]. The CACTUS energy threshold is around 50 GeV, and no statistically significant excess for energies greater than 150 GeV was reported.

Given several potential issues concerning the effect of the integrated starlight from the background and from Draco’s stars, the noise-reduction procedures, and the intrinsic background related to misidentified electromagnetic showers induced by hadrons and electrons, it is extremely difficult to reliably estimate the *signal* gamma-ray flux from Draco. Some portion of the excess counts over the background reported by CACTUS will presumably not be related to the putative dark-matter signal. It seems reasonable to assume that the gamma-ray flux is bracketed between two extremes: as a conservative upper limit, one can consider the overall *excess* counts detected from the angular region of 1 degree centered around Draco above the average background measured outside Draco, which cor-

responds to approximately 30,000 photons, detected with an effective area of the order of  $5 \times 10^4 \text{ m}^2$  in 7 hours of observation [16]. (This procedure was applied in the recent analysis of Ref. [18].)

As an alternative, we can proceed as if the experiment had an angular resolution of 0.1 degrees. Currently, the angular resolution toward Draco is not yet well understood by the CACTUS collaboration. A point-source resolution of 0.3 degrees was obtained toward the Crab nebula, but the resolution toward Draco may be even poorer. It is thus premature to attribute the 1 degree spread in the Draco excess to a source of a 1-degree spatial extent; it may well still be consistent with a point source. Still, to illustrate the possibilities with future measurements with better resolution, we proceed with our theoretical investigation as if the experiment had such a resolution. In this illustrative exercise, one can then suppose that the signal comes only from the innermost 0.1 degree angular region around the center of Draco, and that the rest of the excess is due to spurious effects. This second procedure is found to be equivalent, in the estimate of the signal flux, to requiring that in the innermost region of Draco, which should contain most of the dark-matter-induced gamma-ray flux, the ratio of the signal over the estimated off-source background for an ACT like CACTUS reproduces the observed relative excess size ( $\approx 20\%$ ) [16].

An angular region  $\Delta\Omega = 10^{-3} \text{ sr}$ , corresponding to an angular radius of approximately 1 degree, gives a signal flux (above the CACTUS energy threshold of 50 GeV) of  $\phi_{-3}^{50} \equiv \phi_\gamma(E_\gamma > 50 \text{ GeV}) \approx 2.4 \div 3.4 \times 10^{-9} \text{ cm}^{-2}\text{s}^{-1}$ , where the lower value corresponds to an effective area  $A_{\text{eff}} = 5 \times 10^4 \text{ m}^2$ , while the upper value to an average effective area which takes into account the energy dependence over the interval  $50 < E_\gamma/\text{GeV} < 250$  [16, 18].

In the second approach, based on the innermost 0.1-degree angular region to which an ACT may ultimately be sensitive (corresponding to  $\Delta\Omega \approx 10^{-5} \text{ sr}$ ), the main sources of background correspond to misidentified gamma-like hadronic showers and cosmic-ray electrons. The diffuse gamma-ray background should instead not contribute significantly, but we will take it into account as well. We use the following estimates for the ACT background [5]:

$$\frac{dN_{\text{had}}}{d\Omega}(E > E_0) = 6.1 \times 10^{-3} \epsilon_{\text{had}} \left( \frac{E_0}{1 \text{ GeV}} \right)^{-1.7} \text{ cm}^{-2}\text{s}^{-1}\text{sr}^{-1}, \quad (7)$$

$$\frac{dN_{\text{el}}}{d\Omega}(E > E_0) = 3.0 \times 10^{-2} \left( \frac{E_0}{1 \text{ GeV}} \right)^{-2.3} \text{ cm}^{-2}\text{s}^{-1}\text{sr}^{-1}, \quad (8)$$

$$\frac{dN_{\text{diff}}}{d\Omega}(E > E_0) = 6.7 \times 10^{-7} \left( \frac{E_0}{1 \text{ GeV}} \right)^{-1.1} \text{ cm}^{-2}\text{s}^{-1}\text{sr}^{-1}, \quad (9)$$

where  $\epsilon_{\text{had}} \lesssim 1$  parameterizes the efficiency of hadronic rejection, and where we took for the diffuse gamma-ray background the most conservative differential spectral index (corresponding to the extragalactic gamma-ray background) and normalized the flux to the value of the diffuse emission above 1 GeV from EGRET [30] in the direction of Draco ( $l = 86.4^\circ$ ,  $b = 34.7^\circ$ ). Although the Galactic diffuse



background typically exceeds the extragalactic background at EGRET energies, the two spectra are such that the extragalactic background should dominate above 50 GeV. We therefore derive an overall background level, using an angular acceptance of  $10^{-5}$ sr appropriate for ACTs under our assumptions, of

$$\phi_{\text{bckg}}^{50} \equiv \phi_{\text{bckg}}(E > 50 \text{ GeV}) \simeq 1.2 \times 10^{-10} \text{ cm}^{-2}\text{s}^{-1}, \quad (10)$$

$$\phi_{\text{bckg}}^{150} \equiv \phi_{\text{bckg}}(E > 150 \text{ GeV}) \simeq 1.5 \times 10^{-11} \text{ cm}^{-2}\text{s}^{-1}. \quad (11)$$

Comparing the signal outside Draco and towards its center, the observed excess is around 20% of the background, which gives a putative gamma-ray excess  $\phi_{-5}^{50} \approx 2.4 \times 10^{-11} \text{ cm}^{-2}\text{s}^{-1}$ . We let here the signal vary within one order of magnitude around that central value, to account for the uncertainties in the background estimation and in the actual size of the claimed excess. We therefore consider a signal range, in this approach,  $0.06 \lesssim \phi_{-5}^{50}/\phi_{\text{bckg}}^{50} \lesssim 0.6$ . As mentioned above, this second conservative estimate of the signal is consistent with the actual number of counts reported by CACTUS within an angular radius of around 0.1 degrees.

No excess flux has been observed from Draco above 150 GeV. This leads to a further constraint on the dark-matter interpretation. We consider two putative upper limits: the strongest comes from the requirement that in the central bins the signal is less than 5% of the ACT backgrounds, and reads  $\phi_{-5}^{150} \lesssim 7.5 \times 10^{-13} \text{ cm}^{-2}\text{s}^{-1}$ ; the most conservative requirement is instead that the signal flux does not exceed the Poisson fluctuation of the actual number of counts above the energy threshold of 150 GeV; this gives a limit on the signal flux of  $\phi_{-5}^{150} \lesssim 12.6 \times 10^{-12} \text{ cm}^{-2}\text{s}^{-1}$ .

In the following, we will refer to the CACTUS signal as a photon flux in the range

$$\phi_{-3}^{50} \lesssim 3.4 \times 10^{-9} \text{ cm}^{-2}\text{s}^{-1} \quad \phi_{-5}^{50} \gtrsim 7.2 \times 10^{-12} \text{ cm}^{-2}\text{s}^{-1} \quad \phi_{-5}^{150} \lesssim 0.75 \div 12.6 \times 10^{-12} \text{ cm}^{-2}\text{s}^{-1}. \quad (12)$$

Again, the  $\Delta\Omega = 10^{-5}$  numbers do not describe the current Draco data; rather, they describe results of a hypothetical experiment with 0.1 degree resolution that look like the current CACTUS results.

### 3.1 The gamma-ray angular distribution

The gamma-ray excess is spread over 1 degree. However, given uncertainties in the current CACTUS angular resolution around Draco, we cannot currently use the observed spread to discriminate between a source with a 1 degree spatial extent and a point source. Still, it is conceivable that forthcoming ACT measurements may achieve a resolution as good as 0.1 degrees. In this Section, we illustrate how future such measurements may shed light on the halo profile for Draco. To do so, we proceed as if the resolution of CACTUS were in fact already 0.1 degrees.

Our second estimate of the flux, depending on the assumed dark-matter distribution, and particularly on the scale radius of the dark-matter halo, typically gives a total flux from the central 1 degree

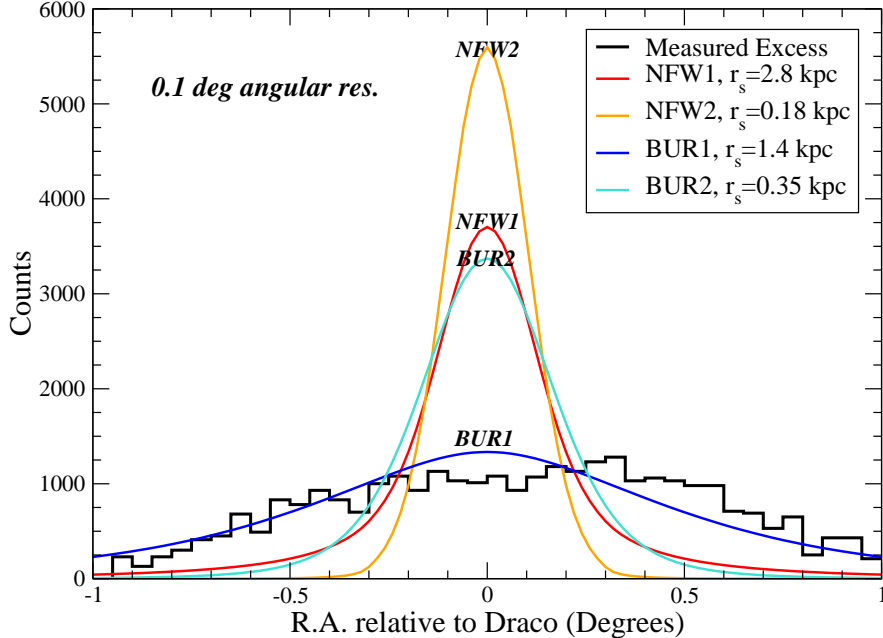


Figure 2: A comparison among theoretical predictions for the angular distribution of the gamma-ray flux from dark-matter annihilation and the excess reported by CACTUS for four different Draco dark-matter halos [19], featuring a wide range of scale radii, and giving consistent  $N$ -body-simulated stellar-velocity dispersions. Keep in mind that the current CACTUS data may have a resolution of roughly one degree, and so conclusions about the Draco halo cannot yet be drawn by comparing the current data with the theoretical curves.

angular region which can be significantly lower than the total counts reported by CACTUS. Within this approach, the counts originating from regions outside the center of Draco would correspond to photons produced by dark-matter annihilation only if a very large scale radius (of the order of 1 kpc) were assumed.

What we will now show is that if CACTUS excess is real and if the Draco halo is cuspy, then an ACT measurement with an 0.1 degree resolution should see a very peaked angular distribution. To do so, we reproduce in Fig. 2 the measured photon excess in the 1-degree angular region centered on the location of Draco. We compare the putative excess with the predictions, for the photon-flux angular distribution, stemming from four different dark-matter halos. We normalize the photon fluxes for the various halos to the total number of excess gamma rays reported by the CACTUS preliminary results. The four profiles were chosen among those quoted in Table 1 of Ref. [19]; two of them are Burkert profiles with scale radii of 1.4 kpc (BUR1, profile B1 in Ref. [19]) and 0.35 kpc (BUR2, profile B2 in Ref. [19]), and two of them are NFW profiles with scale radii of 2.8 kpc (NFW1, profile N1 in Ref. [19]) and 0.18 kpc (NFW2, profile N5 in Ref. [19]). We deduce from Fig. 2 that if the current resolution of CACTUS were as good as 0.1 degrees, then the NFW profiles would produce an excess

of gamma rays in the central bins over what is now seen. If, however, the current angular distribution is still observed even with an 0.1 degree resolution, then cored profiles, with scale radii of order 1 kpc, would be indicated by the data. We conclude therefore that improved angular resolution is warranted to understand better the halo structure.

### 3.2 Implications for particle dark matter

No gamma-ray source in the direction of Draco was identified by EGRET in its all-sky survey. An analysis was carried out by the EGRET collaboration in Ref. [31]. The absence of a point-like source from the direction of Draco can be independently used to draw an upper limit on the integral flux of photons above a threshold of 1 GeV, following the analysis of Ref. [32]. As in Ref. [9], one can take, as the EGRET upper limit on point-like sources gamma-ray fluxes the flux of the least significant point-source detection in the EGRET catalog, corresponding to the Large Magellanic Cloud, which translates into the requirement

$$\phi_{-3}^1 \equiv \phi(E > 1 \text{ GeV}) \lesssim \phi_{\text{EGRET}}^1 \simeq 10^{-8} \text{ cm}^{-2}\text{s}^{-1}. \quad (13)$$

This flux agrees with the theoretical estimate for the flux sensitivity of EGRET to point sources determined in Ref. [33].

The actual EGRET data from the direction of Draco were collected, in Ref. [31], in 7 energy bins, featuring different angular cuts and different exposures. Every energy bin is also accompanied by a background estimate. In order to compare the aforementioned point-source sensitivity of EGRET with the actual photon count, one needs to pick a halo profile for Draco and a signal photon spectrum. We also clustered the four lowest-energy bins ( $0.1 < E_\gamma/\text{GeV} < 1$ ) and the three highest-energy bins ( $1 < E_\gamma/\text{GeV} < 10$ ), since in some bins the background estimate exceeds the photon count, and in the highest-energy bins the statistics are very poor. We require that in the two energy intervals the signal does not exceed the difference between the measured photon counts and the estimated background.

We find that in general the point-source sensitivity agrees, within a factor at most 2, with the bound from the *highest-energy* bins, while that from the *smallest-energy* bins is approximately one order of magnitude weaker (and, in particular, the harder the signal photon spectrum, the weaker the latter bound). The bound from the highest-energy bins tends to be stronger than the point-source-sensitivity constraint for (1) smaller particle masses, (2) for cored rather than cuspy dark-matter halos, and (3) for softer photon spectra. Since, however, the point-source-sensitivity criterion appears to be less dependent on the poor statistics of the highest-energy bins (consisting of only a few photon counts), and since the two criteria essentially agree, we hereafter indicate as the EGRET bound the limit in Eq. (13).

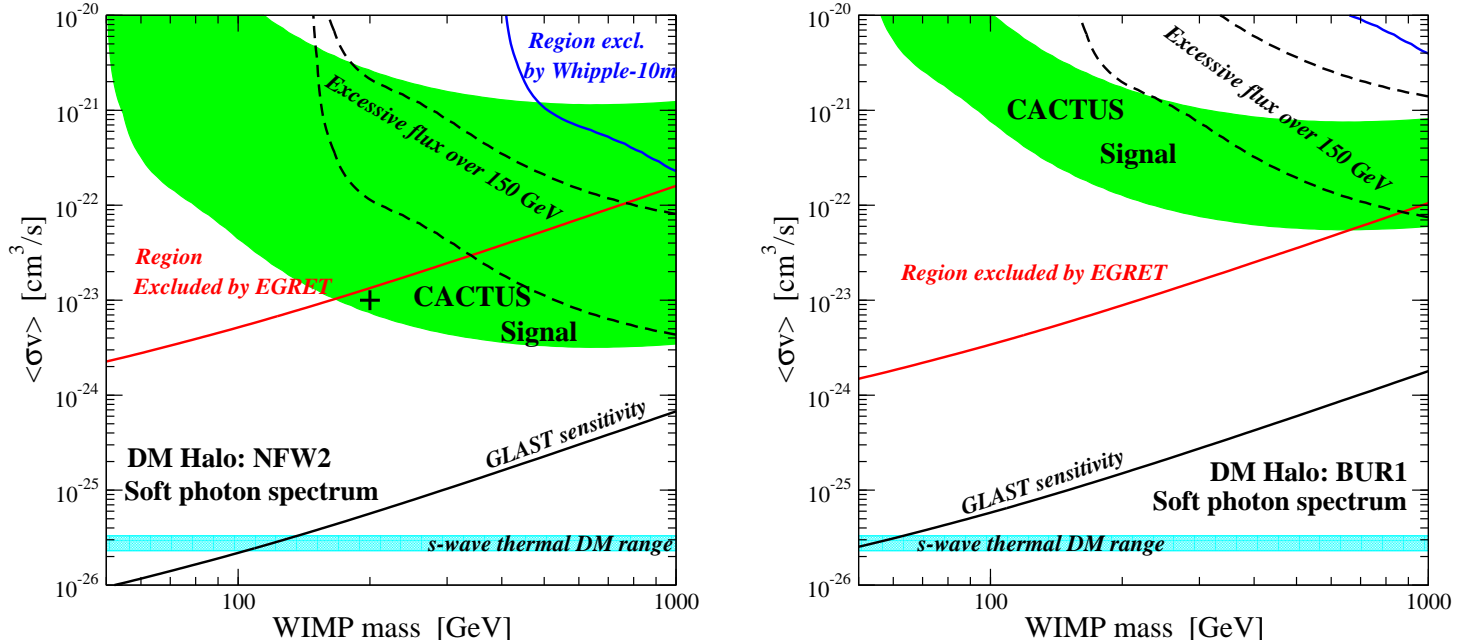


Figure 3: Regions on the  $(m_{\text{WIMP}}, \langle\sigma v\rangle)$  plane compatible with the CACTUS excess and with other observations for a soft photon spectrum (of the same type as that shown with red lines in Fig. 5,  $b\bar{b}$  final state). The two left panels assume the cuspy NFW2 dark-matter halo for Draco, while those on the right the cored BUR1 halo (see Table 1).

The VERITAS collaboration also observed Draco with the Whipple-10m ACT, reporting a null search for high-energy gamma rays above a threshold  $E_\gamma \simeq 400$  GeV, which translates into the bound [34],

$$\phi_{-5}^{400} \equiv \phi(E > 400 \text{ GeV}) \lesssim \phi_{\text{Whipple-10m}}^{400} \simeq 1 \times 10^{-12} \text{ cm}^{-2} \text{ s}^{-1}. \quad (14)$$

The number of gamma rays from the annihilation of a WIMP integrated over an energy  $E_\gamma$  can be written as

$$N_\gamma(E_\gamma) = \int_{E_\gamma}^{\infty} \left( \sum_f \text{BR}(\chi\chi \rightarrow f) \frac{dN_\gamma^f}{dE} \right) dE \quad (15)$$

where the symbol  $f$  refers to any WIMP-annihilation final state, yielding a gamma-ray spectral function (differential number of photons per WIMP annihilation)  $dN_\gamma^f/dE$ . Different final states give different spectral functions. We take here as benchmark cases those giving the hardest and the softest spectra among the final states that are relevant in the case of supersymmetric dark matter; i.e.,  $\tau^+\tau^-$  and  $b\bar{b}$ , respectively.

We show in Figs. 3 and 4 the region, on the  $(m_{\text{WIMP}}, \langle\sigma v\rangle)$  plane, compatible with the putative CACTUS signal quoted in Eq. (12), and the various constraints discussed above, including the two

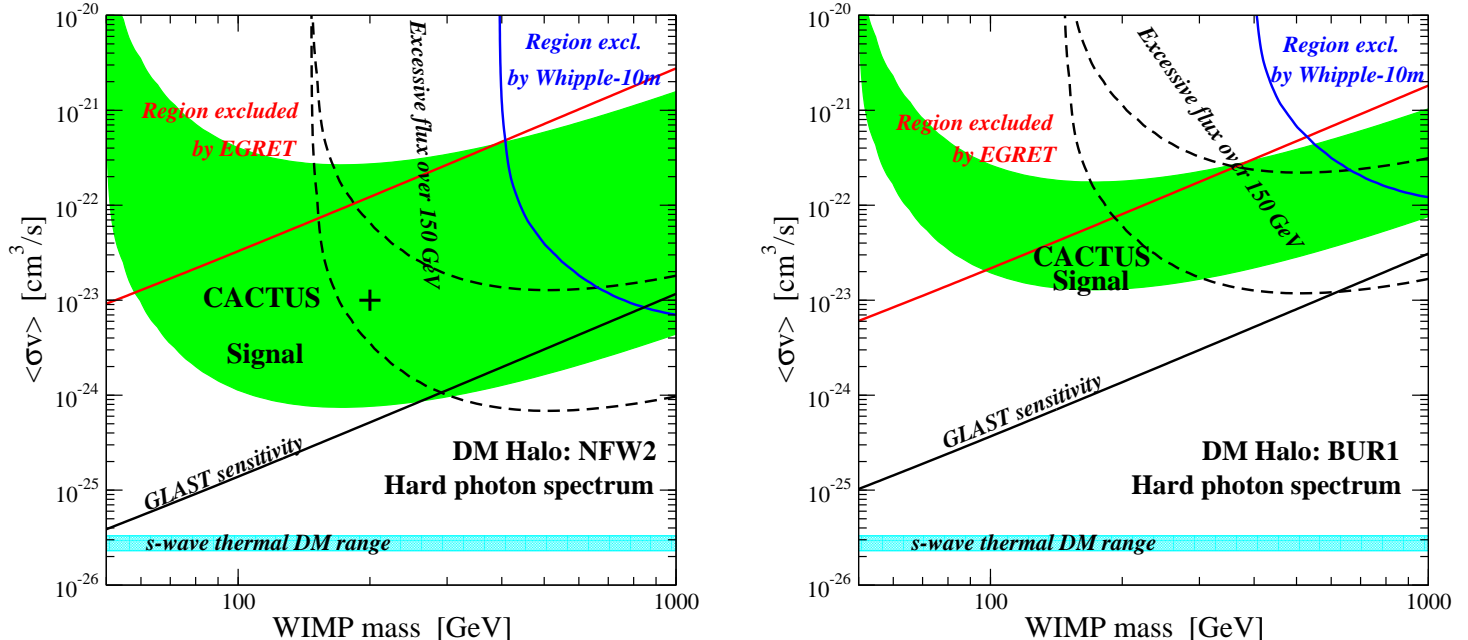


Figure 4: As in Fig. 3, but for a hard photon spectrum (blue dashed lines in Fig. 5,  $\tau^+\tau^-$  final state).

estimates of the limit from the non-observation of a significant excess of gamma rays with energies above 150 GeV. Fig. 3 refers to a soft photon spectrum, corresponding to the final state  $f = b\bar{b}$ , while Fig. 4 to a hard photon spectrum,  $f = \tau^+\tau^-$ . The two panels to the left to a cuspy profile (namely, the NFW2 profile, i.e. profile N5 in Ref. [19]), while the two panels to the right employ a cored dark-matter halo (namely, the BUR1 profile; i.e., profile B3 in Ref. [19]).

We emphasise how the range of dark-matter annihilation cross sections needed to explain the CACTUS signal is largely above what a naive estimate from the thermal production of relic WIMPs would suggest. Assuming that the pair annihilation rate  $\langle\sigma v\rangle$  is energy independent, and therefore that annihilations proceed through  $s$ -wave processes, the WIMP  $\chi$  relic abundance scales as  $\Omega_\chi h^2 \simeq 3 \times 10^{-27} \text{ cm}^3 \text{ s}^{-1} / \langle\sigma v\rangle$  [1]. Requiring that all the CACTUS excess originates from dark-matter annihilations would therefore naively entail thermal relic abundances as low as  $\Omega_\chi h^2 \sim 10^{-5} \div 10^{-6}$ . For reference, we indicate the  $\langle\sigma v\rangle$  range deduced from the previous relation and from the  $2\text{-}\sigma$  WMAP estimate of the CDM abundance [41] with light blue bands in fig. 3 and 4. Resonant annihilations, coannihilation processes or thresholds can significantly distort, though, the above outlined estimate: we postpone to sec. 3.3 (see in particular fig. 8) a discussion of the compatibility of the CACTUS signal with the thermal production of dark matter for the particular case of neutralinos.

We also include the sensitivity of GLAST, computed assuming a total exposure of  $3.2 \times 10^{11} \text{ cm}^2 \text{ s}$  and the diffuse gamma-ray background measured by EGRET, Eq. (9), and requiring the strongest

among the following conditions: (1)  $N_S/\sqrt{N_B} > 5$ ,  $N_S$  and  $N_B$  being the total number of signal and background events, or (2)  $N_S > 10$ . The angular acceptance was set to maximize the signal-to-noise ratio (namely, the quantity  $J_{\Delta\Omega}\sqrt{\Delta\Omega}$  for a given halo profile) between the minimal angular resolution and the maximal field of view.

In the case of a soft photon spectrum (Fig. 3), the EGRET bound rules out large parts of the CACTUS signal, regardless of the assumed halo profile. With a soft photon spectrum, all models consistent with the lower estimate of the CACTUS signal will be largely within the GLAST sensitivity.

With a hard signal photon spectrum (Fig. 4), the bound from the Whipple-10m observation of Draco is significantly more effective than with a soft spectrum; again, almost all the region compatible with the CACTUS signal will be within GLAST reach. We also remark that with the BUR1 profile (Fig. 4, right), and with a hard photon spectrum, we find models that (1) give a total photon flux equal to the CACTUS counts; (2) give an angular distribution of the photon counts that is very close to that reported by CACTUS (see Fig. 2; keep in mind that the theoretical curves reported in Fig.2 refer to a much better angular resolution than that of CACTUS); and (3) are consistent with the conservative criterion on the gamma-ray flux above 150 GeV.

The two black crosses indicate two benchmark points, whose differential photon spectrum is reproduced in Fig. 5 for illustrative purposes, together with the expected diffuse gamma-ray background, for a space-based gamma-ray telescope with angular resolution  $\Delta\Omega = 10^{-3}$  sr (EGRET-like) and  $\Delta\Omega = 10^{-5}$  sr (GLAST-like). We also show the monochromatic gamma-ray line, assuming  $\langle\sigma v\rangle_{\gamma\gamma}/\langle\sigma v\rangle_{\text{tot}} = 3 \times 10^{-4}$  (close to the maximal value for supersymmetric dark matter; see Sec. 3.4), and different energy resolutions, appropriate for the two space-based detectors.

### 3.3 Supersymmetric dark matter

Our analysis was based, up to this point, on a model-independent approach as far as the annihilation cross section and the final-state branching ratio for dark-matter annihilation are concerned. In order to predict the rates for dark-matter detection in other search arenas, such as direct detectors and  $\text{km}^3$  neutrino telescopes, one needs to consider specific particle models. To this extent, we now specialize to supersymmetric dark matter and consider the minimal  $CP$ -conserving supersymmetric extension of the standard model (MSSM), and perform a random scan over its parameter space. For all models, we impose constraints from direct supersymmetric-particles searches at accelerators, rare processes with a sizeable potential supersymmetric contribution, the lower bound on the mass of the lightest  $CP$ -even Higgs boson, and precision electroweak tests. We also require the lightest supersymmetric particle (LSP) to be the lightest neutralino. We do not, however, require that the thermal relic abundance  $\Omega_\chi$  of the LSP falls within the CDM abundance determined within the  $\Lambda$ CDM paradigm. We assume that non-thermal production of neutralinos in the early Universe [35], or cosmological enhancements of the

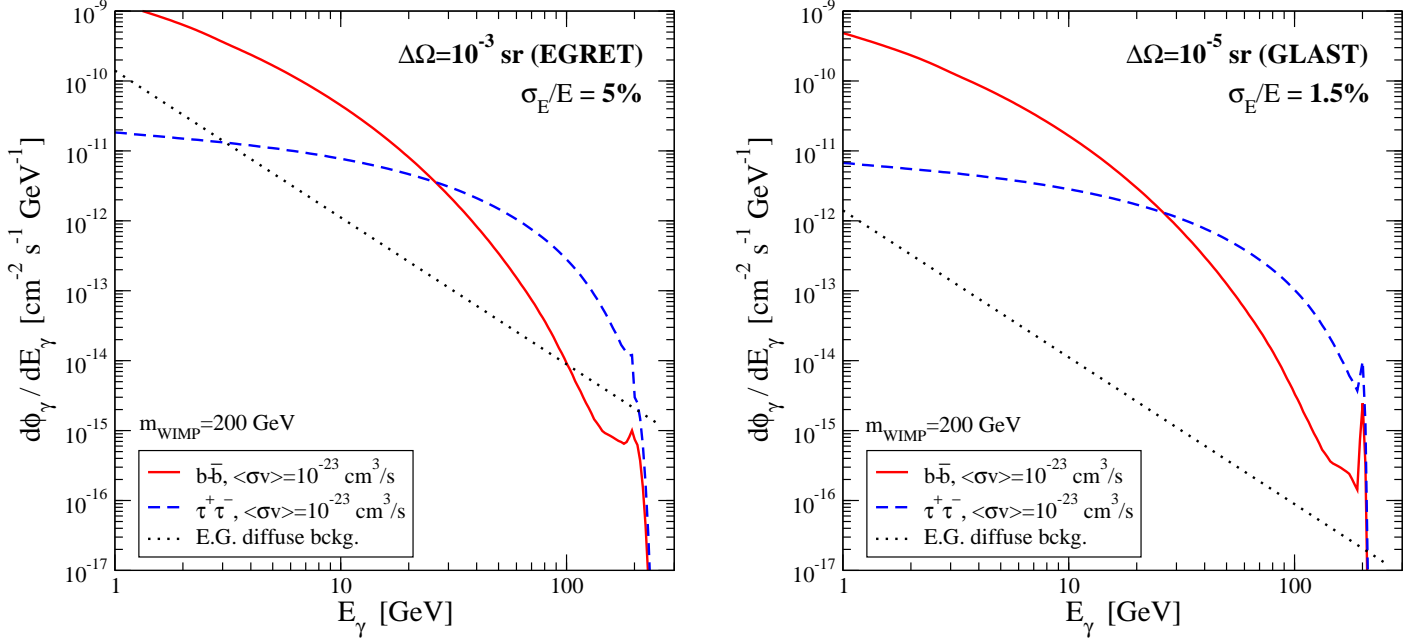


Figure 5: *Sample soft (solid red lines,  $b\bar{b}$  final state) and hard (dashed blue lines,  $\tau^+\tau^-$  final state) photon spectra giving a photon flux compatible with the excess observed from the direction of Draco by the CACTUS ACT. The WIMP mass is set to 200 GeV, and the annihilation cross section times velocity to  $\langle\sigma v\rangle = 10^{-23} \text{ cm}^3\text{s}^{-1}$ . The dotted lines correspond to an estimate of the diffuse gamma-ray background, and the left panel refers to an angular resolution  $\Delta\Omega = 10^{-3} \text{ sr}$ , while the right panel to an angular resolution  $\Delta\Omega = 10^{-5} \text{ sr}$ , with the assumed NFW2 dark-matter halo.*

$\mu$	$m_1$	$m_2$	$m_3$	$m_A$	$m_{\tilde{S}}$	$A_{\tilde{S}_3}$	$\tan\beta$
$30 \div 1200$	$2 \div 1200$	$50 \div 1200$	$m_{\text{LSP}} \div 20000$	$100 \div 10m_{\text{LSP}}$	$(1 \div 10)m_{\text{LSP}}$	$(-3 \div 3)m_{\tilde{S}}$	$1 \div 60$

Table 2: *Ranges of the MSSM parameters used to generate the models shown in Figs. 6 and 8. All masses are in GeV, and  $m_{\text{LSP}} \equiv \min(\mu, m_1, m_2)$ . The quantity  $m_{\tilde{S}}$  indicates the following scalar masses (which were independently sampled):  $m_{\tilde{Q}_{1,3}}, m_{\tilde{u}_{1,3}}, m_{\tilde{d}_{1,3}}, m_{\tilde{L}_{1,2,3}}, m_{\tilde{e}_{1,2,3}}$ . To avoid FCNC constraints, we assumed the squark soft supersymmetry breaking terms of the first two generations to be equal.  $A_{\tilde{S}_3}$  stands for the third generation sfermion trilinear terms: those of the first two generations were taken to vanish.*

relic neutralino density [36], brought  $\Omega_\chi \simeq \Omega_{\text{CDM}}$ . We detail in Table 2 the MSSM scan procedure.

In the upper left panel of Fig. 6, we indicate on the  $(m_\chi, \langle\sigma v\rangle)$  plane supersymmetric models that give a gamma-ray flux from Draco in the range of Eq. (12). Filled points are also consistent with the (strongest) requirement of a sufficiently low gamma-ray flux above 150 GeV. All models are consistent, instead, with the conservative constraint, from the Poisson variance of the measured counts, on the flux above 150 GeV. We employ here the BUR2 profile of Table 1. We also indicate the regions that significantly improve the fit to the gamma-ray flux from the direction of the Galactic center

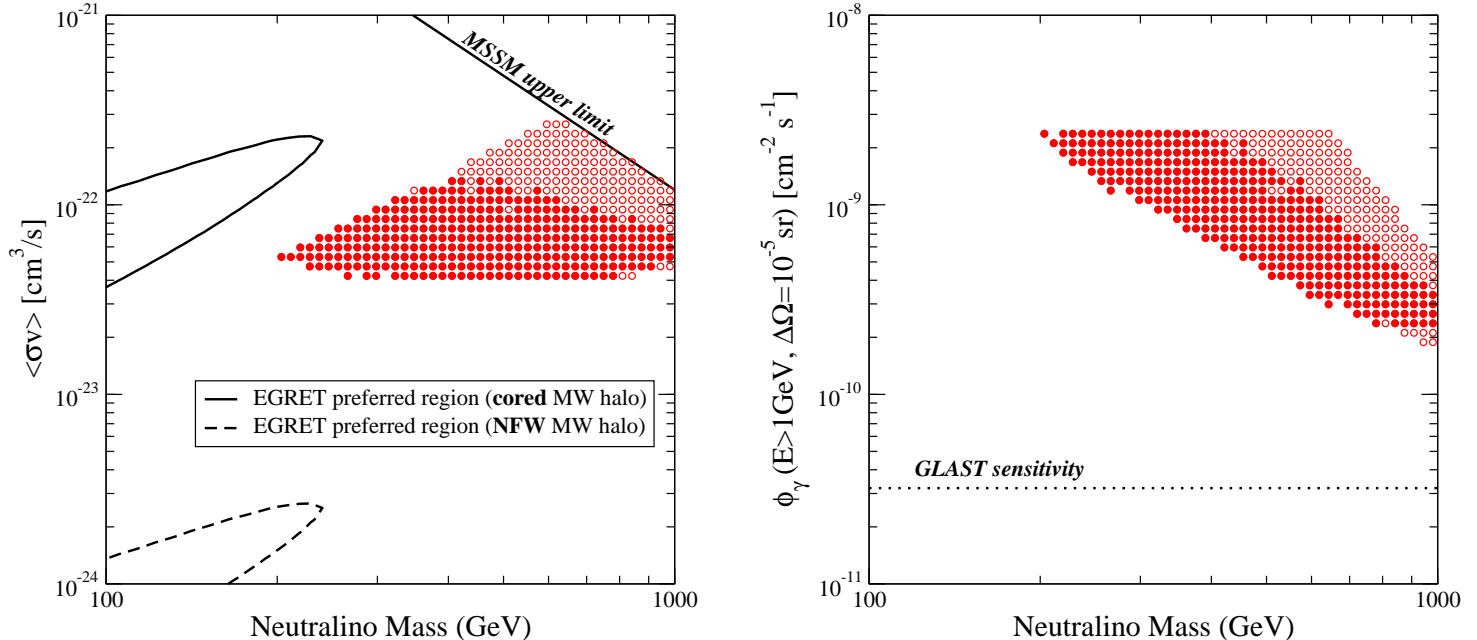


Figure 6: We show the results of a scan over the general MSSM (see Table 2 for details) where we looked for supersymmetric models providing a flux of gamma rays from Draco compatible with the CACTUS excess. The left panel shows the  $(m_{\text{WIMP}}, \langle\sigma v\rangle)$  plane, while the right panel shows the expected integral flux of photons at GLAST, with the corresponding estimated point-source sensitivity in the direction of Draco.

as measured by EGRET [37], for a cored and an NFW Milky Way dark-matter halo. Intriguingly enough, for a Milky Way halo that is slightly cuspier than a Burkert (cored) profile (solid black line in Fig. 6, right), the region favored by the EGRET data can be consistent with the Draco signal, provided the neutralino mass is not much heavier than 250 GeV. We also indicate the upper limit on the annihilation cross section in the general MSSM derived in Ref. [8], and note that most models fall very close to the maximal cross sections in the context of supersymmetric dark matter. Such large cross sections could be in conflict with the production of other secondary annihilation products, such as antiprotons, positrons, or antideuterons [38, 39]. However, the large uncertainties in the modeling of diffusion processes and nuclear reactions, together with those connected to the Milky Way dark-matter halo, can leave the freedom to circumvent those constraints [39].

We find that over the whole scanned supersymmetric parameter space, the total flux over the whole 1 degree angular region features, with the BUR2 profile we employ here, an upper limit  $\phi_{-3}^{50} \lesssim 2 \times 10^{-10}$ , with a maximum at a neutralino mass of 600 GeV. This upper bound indicates that no supersymmetric



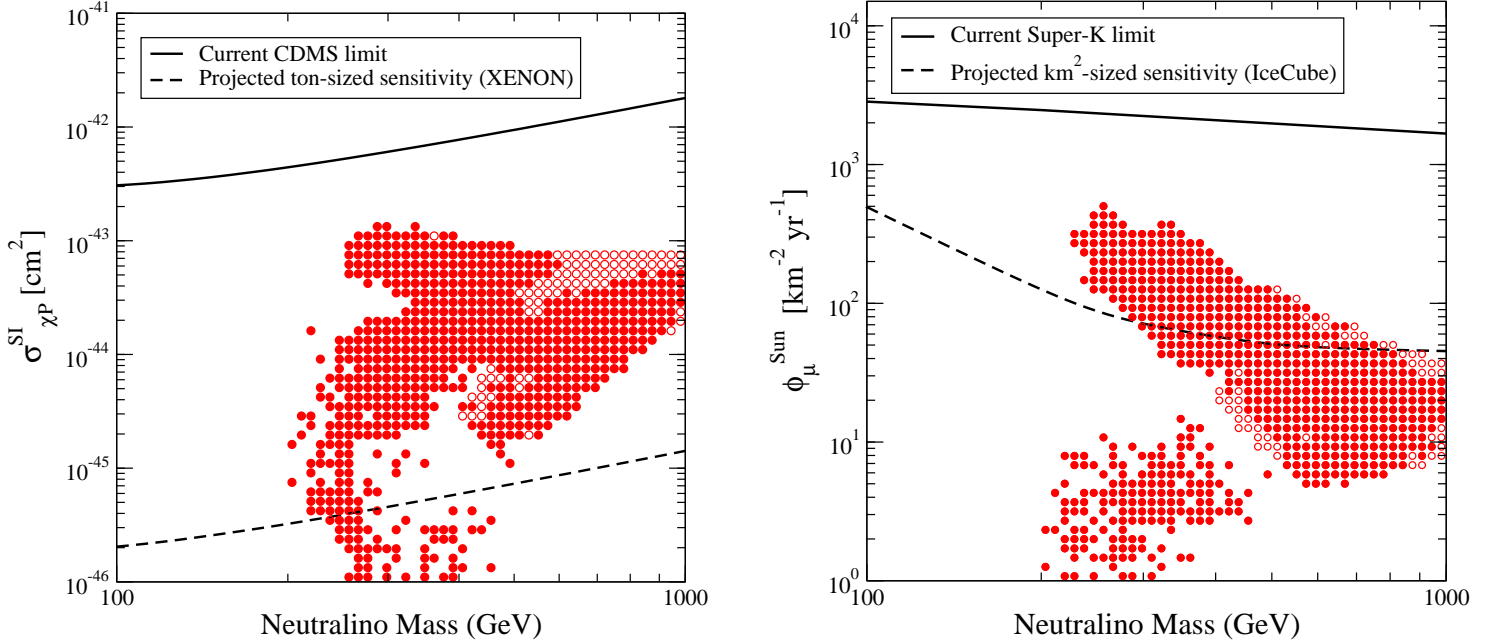


Figure 7: *The neutralino-proton scalar-interaction cross section and the flux of muons from the Sun induced by neutralino annihilations, with the corresponding present and future experimental sensitivities, for the same models as in Fig. 6.*

models can give, in the present halo setup, 100% of the excess counts over the off-source background detected by CACTUS. The latter could be achieved with a cuspier NFW profile, the scaling among the fluxes simply being  $\phi^{\text{NFW}}/\phi^{\text{BUR}} = J^{\text{NFW}}/J^{\text{BUR}}$  (see Fig. 1).

We then carry out an analysis of the prospects for the detection of the CACTUS-compatible supersymmetric models with other search avenues. In particular, in the right panel of Fig. 6, we show the total photon flux expected at GLAST, integrated over an energy threshold of 1 GeV, and with  $\Delta\Omega = 10^{-5}$  sr (which maximizes the signal to noise with the profile we use here). All CACTUS-compatible supersymmetric models will be, under the present assumptions, unambiguously within the sensitivity of GLAST. The upper bound on the integrated flux of photons stems from the EGRET bound, Eq. (13), since  $\phi^{\text{GLAST}} = 10^{-2}\phi^{\text{EGRET}}(J_{-5}/J_{-3}) \approx 2.3 \times 10^{-9} \text{ cm}^{-2}\text{s}^{-1}$ .

Fig. 7 collects, again for the CACTUS-compatible supersymmetric models discussed above, the results for the rates at future direct-detection experiments (left) and at IceCube (right), where muons induced by neutrinos from dark-matter annihilation in the Sun will be sought. Although not guaranteed, the detection prospects for supersymmetric models featuring the correct mass and annihilation cross sections certainly look promising.

If we require the thermal neutralino relic abundance to agree with the CDM abundance, then

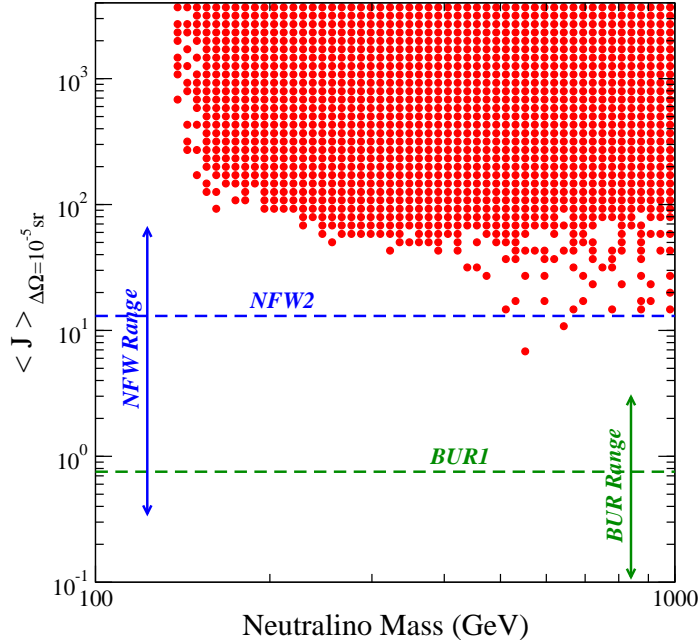


Figure 8: Scan of the general MSSM (see Table 2) showing the putative values of  $J_{-5}$  needed to explain the CACTUS excess for supersymmetric models featuring a thermal relic abundance  $\Omega_\chi h^2 \simeq \Omega_{\text{CDM}} h^2$ . The horizontal lines indicate the values of  $J_{-5}$  for a sample of Draco halo profiles [13], including the NFW2 and BUR1 profiles of Figs. 3 and 4.

strong constraints are placed to the range of annihilation cross sections. One can then ask, for neutralino models with the correct thermal abundance, what values of  $J_{-5}$  are required to account for the CACTUS excess? We answer this question in Fig. 8, where we indicate, for MSSM models obtained in the same scan outlined in Table 2 that fulfill the condition  $\Omega_\chi \simeq \Omega_{\text{CDM}}$ , the values of  $J_{-5}$  such that  $\phi_{-5}^{50} = 2.4 \times 10^{-11} \text{ cm}^{-2} \text{ s}^{-1}$ . We show with vertical lines the values of  $J_{-5}$  for the profiles employed in Figs. 3 and 4. The vertical arrows indicate the overall ranges for  $J_{-5}$  obtained in the analysis of Sec. 2. Evidently, even the minimal gamma-ray flux compatible with the CACTUS excess requires an extremely cuspy halo for Draco. As we pointed out before, such cuspy profiles should be readily identifiable once a better angular resolution is achieved through the analysis of the angular distribution of the photon excess counts.

### 3.4 Monochromatic gamma rays

Given the preliminary spectral structure of the CACTUS Draco gamma-ray excess—i.e. a large amount of counts in a narrow energy range—it is certainly worthwhile to investigate whether the excess may be due to direct annihilation of dark-matter particles to photons. Unfortunately, the poor energy resolution of the solar-array ACT is not suitable for a prompt discrimination of this possibility, which, if

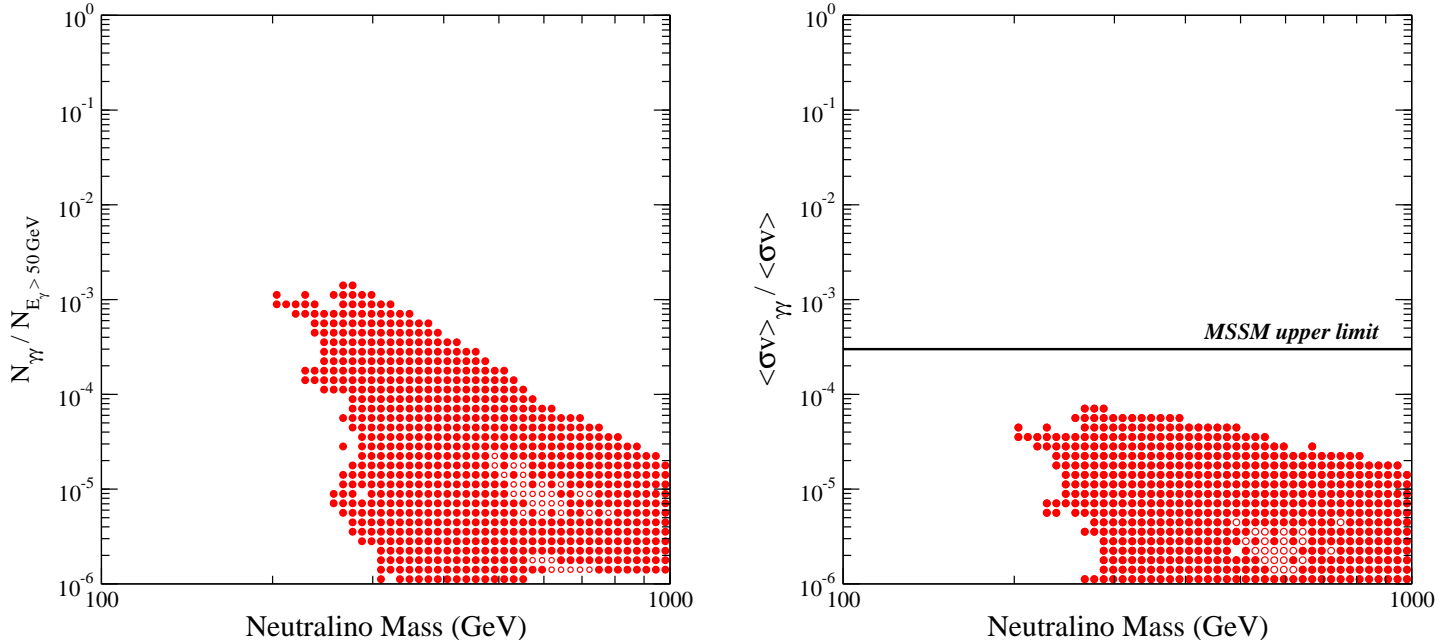


Figure 9: *Left:* The ratio between the number of photons from direct pair annihilation of neutralinos into two photons and from the gamma-ray continuum, integrated above 50 GeV, for the CACTUS-compatible supersymmetric models of Fig. 6. *Right:* the ratio of the annihilation cross section of neutralinos into two photons over the total neutralino annihilation cross section, for the same ensemble of models.

detected, would constitute a smoking gun for dark-matter annihilation. A dominantly monochromatic signal would moreover circumvent the friction with the EGRET null result.

As a first step, we again consider here supersymmetric dark matter, and determine whether a scenario where the bulk of the dark-matter-induced gamma-ray flux originates from direct neutralino annihilation into two photons is at all viable. To this extent, we show in the left panel of Fig. 9 the relative fraction of monochromatic photons versus the integrated number of continuum photons with energies larger than 50 GeV, for supersymmetric models giving a CACTUS-compatible gamma-ray flux, as determined in the previous Section. In the right panel, we show the relative branching fraction for neutralino annihilation into photons. We conclude that within supersymmetric models, the bulk of the photon flux always stems from the continuum component, the monochromatic part contributing less than  $\approx 0.2\%$  of the photon counts for CACTUS-compatible supersymmetric models. As a byproduct, we derived from the full scan an upper bound on the branching ratio of neutralino annihilation into two photons in the general MSSM which reads

$$r \equiv \langle\sigma v\rangle_{\gamma\gamma}/\langle\sigma v\rangle_{\text{tot}} \lesssim 3 \times 10^{-4}. \quad (16)$$

On more general grounds, outside the supersymmetric paradigm, one can still hypothesize that the

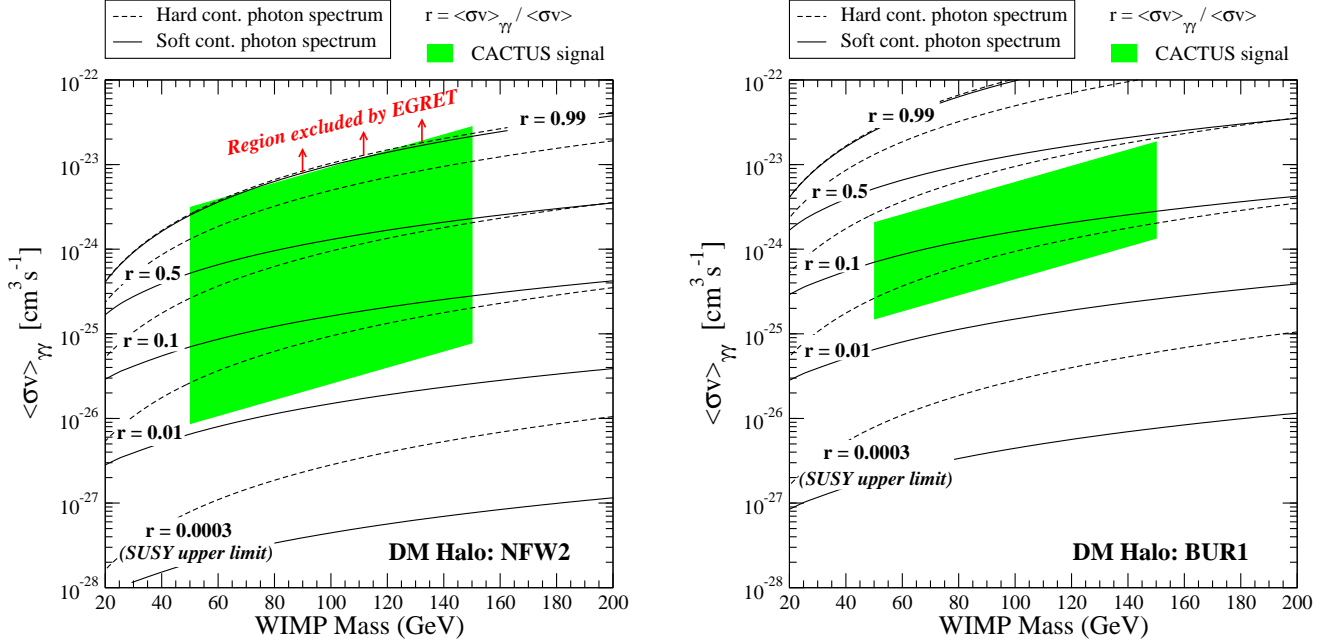


Figure 10: Limits in the  $(m_\chi, \langle\sigma v\rangle_{\gamma\gamma})$  plane to the ratio  $r \equiv \langle\sigma v\rangle_{\gamma\gamma} / \langle\sigma v\rangle_{\text{tot}}$  from the EGRET bound on the low-energy gamma-ray flux from Draco, for the cuspy NFW2 profile (left) and for the cored BUR1 profile (right), and for soft (solid lines) and hard (dashed lines) continuum photon spectra.

bulk of the CACTUS signal comes from the monochromatic line, and constrain, through the EGRET bound, the continuum contribution, and hence the quantity  $r$ . We point out that the  $Z\gamma$  or the  $Zh$  lines would constitute less favorable scenarios here, since (1) the monochromatic photon flux would be smaller by a factor 0.5, and (2) the continuum photons from the  $Z$  and  $h$  decay would contribute to the continuum photon yield, strengthening the EGRET bound.

We assume, in Fig. 10, hard and soft photon spectra (dashed and solid lines: the regions lying above the lines are excluded by the EGRET constraint), and cuspy and cored profiles for the Draco dark-matter halo (left and right panels). The green regions correspond to the CACTUS signal: in the case of a cored profile, the branching ratio into two photons must be at least as large as  $1 \div 10\%$ , clearly incompatible with supersymmetric dark matter. Requiring that all of the CACTUS excess counts originate from photons produced in dark-matter annihilation, and consistency with the EGRET bound, implies much larger branching fractions ( $r \simeq 0.5 - 0.99$ ) and a dark-matter model where the dark-matter particle predominantly annihilates into two photons.

### 3.5 Decaying dark matter

Uncertainties in the innermost structure of dark-matter halos critically impact the computation of the flux of photons from dark-matter annihilation. Since the annihilation rate per unit volume is proportional to the square of the dark-matter density, the occurrence of high-density spikes or cusps in the center of dark-matter halos may lead to flux enhancements of various orders of magnitude, without affecting significantly the outer structure of the dark halo, where the rotation curves are usually best determined. If, alternatively, the gamma-ray excess results from the *decay* of a quasi-stable dark-matter particle, the flux is only linearly proportional to the dark matter density (and hence, in the case of a distant object like Draco, to a first approximation, to the total dark-matter mass), which is much more reliably constrained by dynamical measurements, inducing a significantly smaller spread in the flux predictions.

We now show that the CACTUS Draco gamma-ray excess *cannot* be explained in terms of a decaying dark-matter particle. The resulting flux of photons in the diffuse gamma-ray background and from the center of our own Galaxy would in fact be exceedingly large. The ratio of the gamma-ray flux  $\phi^{\text{Draco}}$  from Draco's halo and that  $\phi^{\text{MW}}$  from the Milky Way halo can be written as

$$r_{\text{GC, DB}} \equiv \frac{\phi^{\text{Draco}}}{\phi_{\text{GC, DB}}^{\text{MW}}} \simeq \left( \frac{M_{\text{DM}}^{\text{Draco}}}{(d^{\text{Draco}})^2} \right) \left( \int_{\text{line of sight}} \rho^{\text{MW}}(l) dl \right)^{-1}, \quad (17)$$

where the line-of-sight integral is performed either in the direction of the Galactic center ( $r_{\text{GC}}$ ) or in the direction of Draco, to evaluate the diffuse gamma-ray background ( $r_{\text{DB}}$ ). If the Draco mass is formed entirely by dark matter, then  $M_{\text{DM}}^{\text{Draco}} \simeq 8.6 \times 10^7 M_{\odot}$  [25]. The distance to Draco is  $d^{\text{Draco}} \simeq 76$  kpc [40]. The Milky Way line-of-sight integrals depend on the assumed dark-matter halo. We evaluated the integrals for two extreme choices, a NFW profile [20] with scaling density and radius  $\rho_s = 5.4 \times 10^6 M_{\odot}/\text{kpc}^3$  and  $r_s = 21.8$  kpc respectively, and a Burkert profile [29], with scaling density and radius  $\rho_s = 1.5 \times 10^7 M_{\odot}/\text{kpc}^3$  and  $r_s = 11.7$  kpc. We find

$$r_{\text{DB}} \lesssim 1.5 \div 1.7 \times 10^{-4}, \quad r_{\text{GC}} \lesssim 0.25 \div 68 \times 10^{-6}, \quad (18)$$

with the smaller figures corresponding to the NFW Milky Way profile. Over a 1 degree angular region, the diffuse gamma-ray background from the direction of Draco quoted in Eq. (9) gives an integrated flux over 50 GeV  $\phi_{\text{DB}}^{50} \lesssim 10^{-11} \text{ cm}^{-2}\text{s}^{-1}$ . We do not have a direct measurement of the gamma-ray spectrum from the Galactic center in the energy window between 10 GeV and 150 GeV, the lower limit being the highest energy probed by EGRET, and the upper limit the lowest energy probed by HESS. To have an idea of the integral flux above 50 GeV one can extrapolate the power-law behaviors featured by both the EGRET (at  $E \gtrsim 2$  GeV) and HESS differential photon flux, respectively, giving

$$\frac{d\phi_{\text{EGRET}}}{dE} \simeq 1.6 \times 10^{-6} \left( \frac{E}{\text{GeV}} \right)^{-3.1} \text{ cm}^{-2}\text{s}^{-1}\text{GeV}^{-1},$$

$$\frac{d\phi_{\text{HESS}}}{dE} \simeq 2.5 \times 10^{-12} \left( \frac{E}{\text{TeV}} \right)^{-2.2} \text{ cm}^{-2}\text{s}^{-1}\text{TeV}^{-1}.$$

These figures, extrapolated and integrated over the energy range  $E > 50$  GeV, give the following integrated fluxes:

$$\begin{aligned} \phi_{\text{EGRET}}^{50} &\simeq 2 \times 10^{-10} \text{ cm}^{-2}\text{s}^{-1}, \\ \phi_{\text{HESS}}^{50} &\simeq 8 \times 10^{-11} \text{ cm}^{-2}\text{s}^{-1}. \end{aligned}$$

The flux of gamma-ray photons from dark-matter decay from Draco is therefore conservatively bounded to be

$$\begin{aligned} \phi_{\text{Draco}}^{50} &\lesssim 1.7 \times 10^{-15} \text{ cm}^{-2}\text{s}^{-1}, & \text{diffuse gamma - ray background,} & (19) \\ \phi_{\text{Draco}}^{50} &\lesssim 1.4 \times 10^{-14} \text{ cm}^{-2}\text{s}^{-1}, & \text{Galactic center,} & (20) \end{aligned}$$

which is clearly incompatible with the estimates in Eq. (12).

We therefore conclude that the expected flux from the Galactic center and from the diffuse gamma-ray background are not consistent with the putative CACTUS signal from Draco in the context of a decaying dark-matter particle. A sufficiently large Draco flux would evidently violate the available constraints to the diffuse gamma-ray background and on the flux of gamma rays from the center of the Milky Way by various orders of magnitude.

## 4 Conclusions

We considered in this paper the possibility that the gamma-ray excess observed by CACTUS from the direction of the Draco dSph galaxy originates from WIMP annihilation. We summarize below the main results of the present analysis:

- We showed that future measurements, with  $\sim 0.1$  degree angular resolution, should allow us to distinguish between cored and cuspy halos, even though the current CACTUS angular resolution is not good enough.
- We estimated the putative gamma-ray flux from dark-matter annihilation considering the two extreme possibilities that the dark-matter signal consists of (1) all the excess counts reported by CACTUS, and (2) the excess over background corresponding to Draco's innermost region.
- We analyzed, in a model-independent approach, the regions of the particle-mass versus annihilation-cross-section parameter space compatible with the estimated CACTUS excess, imposing the constraints from the null results of gamma-ray searches reported by EGRET and by the VERITAS

collaboration observation with the Whipple-10m ACT, and from the absence of a statistically relevant excess in the CACTUS data for photon energies above 150 GeV. The annihilation cross section range lies well above that expected with standard thermal relic dark matter production.

- The total excess counts over background reported by CACTUS can only be reproduced with a very cored dark-matter halo and a hard photon spectrum. If this is the correct explanation for the excess, then higher-angular-resolution measurements should still show a  $\sim 1$  degree spread around Draco's center. Almost all CACTUS-compatible models will be within reach of GLAST.
- In the case of supersymmetric dark matter, the annihilation cross sections needed to reproduce the CACTUS signal are close to the maximal theoretically allowed values and would imply a negligible thermal relic abundance. CACTUS-compatible supersymmetric models give typically very large detection rates at direct-detection experiments, and a sizeable neutrino flux from neutralino annihilation in the Sun, which in principle could allow a cross-check of the gamma-ray signal that GLAST should see within this scenario.
- The possibility of a dominantly monochromatic origin of the CACTUS excess is not viable within supersymmetry, and requires, for consistency with the EGRET null result from Draco, dark-matter models that annihilate predominantly to two photons and thus produce a very suppressed continuum photon spectrum.
- A decaying-dark-matter scenario is ruled out by the resulting inferred gamma-ray flux from the center of the Milky Way and in the diffuse gamma-ray background.

## Acknowledgments

We would like to thank Max Chertok, Francesc Ferrer, Jeter Hall, Reshmi Mukherjee, Mani Tripathi, and Piero Ullio for helpful discussions. This work was supported in part by DoE DE-FG03-92-ER40701 and FG02-05ER41361 and NASA NNG05GF69G.

## References

- [1] G. Jungman, M. Kamionkowski and K. Griest, Phys. Rept. **267** (1996) 195 [arXiv:hep-ph/9506380].
- [2] L. Bergström, Rept. Prog. Phys. **63**, 793 (2000) [arXiv:hep-ph/0002126]; G. Bertone, D. Hooper and J. Silk, Phys. Rept. **405**, 279 (2005) [arXiv:hep-ph/0404175].
- [3] W. Atwood *et al.* [GLAST-LAT Collaboration], *Prepared for 11th International Conference on Calorimetry in High-Energy Physics (Calor 2004), Perugia, Italy, 28 Mar - 2 Apr 2004*

- [4] F. A. Aharonian and C. W. Akerlof, *Ann. Rev. Nucl. Part. Sci.* **47** (1997) 273; F. Aharonian, arXiv:astro-ph/0511139;
- [5] L. Bergström, P. Ullio and J. H. Buckley, *Astropart. Phys.* **9**, 137 (1998) [arXiv:astro-ph/9712318].
- [6] W. de Boer, C. Sander, A. V. Gladyshev and D. I. Kazakov, arXiv:astro-ph/0508617.
- [7] D. Hooper, I. de la Calle Perez, J. Silk, F. Ferrer and S. Sarkar, *JCAP* **0409**, 002 (2004) [arXiv:astro-ph/0404205]; D. Horns, *Phys. Lett. B* **607**, 225 (2005) [Erratum-ibid. B **611**, 297 (2005)] [arXiv:astro-ph/0408192]; D. Hooper and J. March-Russell, *Phys. Lett. B* **608**, 17 (2005) [arXiv:hep-ph/0412048].
- [8] S. Profumo, *Phys. Rev. D* **72** (2005) 103521 [arXiv:astro-ph/0508628].
- [9] C. Tyler, *Phys. Rev. D* **66** (2002) 023509 [arXiv:astro-ph/0203242].
- [10] E. A. Baltz, C. Briot, P. Salati, R. Taillet and J. Silk, *Phys. Rev. D* **61**, 023514 (2000) [arXiv:astro-ph/9909112];
- [11] L. Pieri and E. Branchini, *Phys. Rev. D* **69**, 043512 (2004) [arXiv:astro-ph/0307209]; N. Fornengo, L. Pieri and S. Scopel, *Phys. Rev. D* **70**, 103529 (2004) [arXiv:hep-ph/0407342].
- [12] D. Elsaesser and K. Mannheim, *Phys. Rev. Lett.* **94**, 171302 (2005) [arXiv:astro-ph/0405235];
- [13] N. W. Evans, F. Ferrer and S. Sarkar, *Phys. Rev. D* **69**, 123501 (2004) [arXiv:astro-ph/0311145].
- [14] M.L. Mateo, *ARA&A*, **36**, 435 (1998).
- [15] E.B. Fomalont and B.J. Geldzahler, *Astron. J.* **84**, 12 (1979).
- [16] P. Marleau, TAUP, Zaragoza, Spain, September 2005; M. Tripathi, Cosmic Rays to Colliders 2005, Prague, Czech Republic, September 2005; TeV Particle Astrophysics Workshop, Batavia, USA, July 2005; M. Chertok, proceedings of PANIC 05, Santa Fe, USA, October 2005.
- [17] L.M. Young, *Astron. J.* **117**, 1758 (1999).
- [18] L. Bergström and D. Hooper, arXiv:astro-ph/0512317.
- [19] S. Mashchenko, A. Sills and H.M.P. Couchman, arXiv:astro-ph/0511567.
- [20] J. F. Navarro, C. S. Frenk and S. D. M. White, *Astroph. J.* **499**, L5 (1998) [arXiv:astro-ph/9611107].
- [21] M. Aaronson, *Astroph. J.* **266**, L11 (1983).
- [22] M. Aaronson and E.W. Olszewski (1987) in “Dark Matter in the Universe” (IAU Symposium No.117), eds. J. Kormendy, G.R. Knapp, (Reidel, Dordrecht), p.153; M. Aaronson and E.W. Olszewski (1988) in “Large Scale Structure of the Universe” (IAU Symposium No.130), eds. J. Audouze, M.C. Pelletan, A. Szalay (Kluwer, Dordrecht), p.153.
- [23] T.E. Armandroff, E.W. Olszewski and C. Prior *AJ* **110**, 2131 (1995).
- [24] J.C. Hargreaves, G. Gilmore, M.J. Irwin and D. Carter, *MNRAS* **282**, 305 (1996).



- [25] J. Klenya *et al.*, Ap. J. 563 (2001) L115.
- [26] J. Klenya *et al.*, MNRAS **330**, 792 (2002).
- [27] M.I. Wilkinson *et al.*, ApJ **611**, L21 (2004).
- [28] P. Kroupa, New Astronomy **2**, 139 (1997).
- [29] A. Burkert, Astrophys. J. **447** (1995) L25; P. Salucci and A. Burkert, Astrophys. J. **537** (2000) L9.
- [30] <http://coss.gsfc.nasa.gov/egret/>
- [31] L. Wai, “*Analysis of Draco with EGRET*”,  
<http://www-glast.slac.stanford.edu/ScienceWorkingGroups/DarkMatter/oldstuff/9-9-02.ppt>
- [32] R. C. Lamb and D. J. Macomb, Ap. J. 488 (1997) 872.
- [33] A. Morselli, A. Lionetto, A. Cesarini, F. Fucito and P. Ullio [GLAST Collaboration], Nucl. Phys. Proc. Suppl. **113** (2002) 213 [arXiv:astro-ph/0211327].
- [34] J. Hall, private communication, 2005, and J. Hall [VERITAS Collaboration], arXiv:astro-ph/0507448.  
<http://veritas.sao.arizona.edu/>.
- [35] B. Murakami and J. D. Wells, Phys. Rev. D **64**, 015001 (2001); T. Moroi and L. Randall, Nucl. Phys. B **570**, 455 (2000); M. Fujii and K. Hamaguchi, Phys. Lett. B **525**, 143 (2002); M. Fujii and K. Hamaguchi, Phys. Rev. D **66**, 083501 (2002); R. Jeannerot, X. Zhang and R. H. Brandenberger, JHEP **9912**, 003 (1999); W. B. Lin, D. H. Huang, X. Zhang and R. H. Brandenberger, Phys. Rev. Lett. **86**, 954 (2001);
- [36] M. Kamionkowski and M. S. Turner, Phys. Rev. D **42** (1990) 3310; P. Salati, [arXiv:astro-ph/0207396]; F. Rosati, Phys. Lett. B **570** (2003) 5 [arXiv:hep-ph/0302159]; S. Profumo and P. Ullio, JCAP **0311**, 006 (2003) [arXiv:hep-ph/0309220]; R. Catena, N. Fornengo, A. Masiero, M. Pietroni and F. Rosati, arXiv:astro-ph/0403614; S. Profumo and P. Ullio, Proceedings of the *39th Rencontres de Moriond Workshop on Exploring the Universe: Contents and Structures of the Universe*, La Thuile, Italy, 28 Mar - 4 Apr 2004, ed. by J. Tran Thanh Van [arXiv:hep-ph/0305040].
- [37] H.A. Mayer-Hasselwander *et al.*, Astron. Astrophys. **335** (1998) 161.
- [38] S. Profumo and P. Ullio, JCAP **0407** (2004) 006 [arXiv:hep-ph/0406018].
- [39] H. Baer and S. Profumo, JCAP **0512** (2005) 008 [arXiv:astro-ph/0510722].
- [40] S. Van den Bergh, “*The Galaxies of the Local Group*”, Cambridge, UK: Cambridge University Press, 2000.
- [41] D. N. Spergel *et al.* [WMAP Collaboration], Astrophys. J. Suppl. **148** (2003) 175 [arXiv:astro-ph/0302209].